

# Synthesis of 2-Alkenyl- and 2-Alkynyl-benzo[*b*]phospholes by Using Palladium-Catalyzed Cross-Coupling Reactions

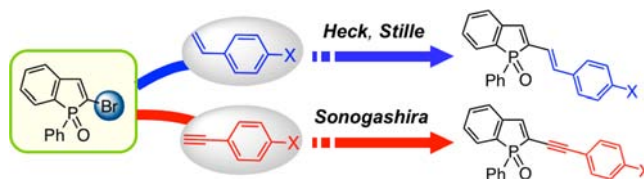
Yoshihiro Matano,<sup>\*,†</sup> Yukiko Hayashi,<sup>‡</sup> Kayo Suda,<sup>§</sup> Yoshifumi Kimura,<sup>||</sup> and Hiroshi Imahori<sup>\*,‡,#</sup>

Department of Chemistry, Faculty of Science, Niigata University, Nishi-ku, Niigata 950-2181, Japan, Department of Molecular Engineering, Graduate School of Engineering, Kyoto University, Nishikyo-ku, Kyoto 615-8510, Japan, Department of Chemistry, Graduate School of Science, Kyoto University, Sakyo-ku, Kyoto 606-8502, Japan, Department of Molecular Chemistry and Biochemistry, Faculty of Science and Engineering, Doshisha University, Kyotanabe 610-0394, Japan, and Institute for Integrated Cell-Material Sciences (WPI-iCeMS), Kyoto University, Nishikyo-ku, Kyoto 615-8510, Japan

matano@chem.sc.niigata-u.ac.jp

Received July 16, 2013

## ABSTRACT



Heck, Stille, and Sonogashira reactions of 2-bromobenzo[*b*]phosphole *P*-oxide afforded a series of 2-alkenyl- and 2-alkynyl-benzo[*b*]phosphole *P*-oxides. The charge-transfer character of the new benzo[*b*]phosphole  $\pi$ -systems in the excited state is enhanced by the terminal electron-donating substituents. Furthermore, the C–Sn cross-coupling of the bromide was applied to the facile synthesis of a new Stille-coupling precursor, 2-stannylbenzo[*b*]phosphole.

Recently, much attention has been paid to phosphole-containing  $\pi$ -systems, which are promising candidates for a new class of phosphorus-based optical and electronic materials.<sup>1</sup> In particular, benzo[*b*]phospholes<sup>2</sup> and related compounds<sup>3–7</sup> have been continuously investigated because of their versatility in the introduction of various

functional groups onto the  $\alpha$  and  $\beta$  carbons of the phosphole unit to extend  $\pi$ -skeletons. Some  $\pi$ -extended and  $\pi$ -fused benzo[*b*]phosphole derivatives are known to

<sup>†</sup> Niigata University

<sup>‡</sup> Graduate School of Engineering, Kyoto University

<sup>§</sup> Graduate School of Science, Kyoto University

<sup>||</sup> Doshisha University

<sup>#</sup> Institute for Integrated Cell-Material Sciences, Kyoto University

(1) For selected reviews, see: (a) Baumgartner, T.; Réau, R. *Chem. Rev.* **2006**, *106*, 4681. Correction: **2007**, *107*, 303. (b) Réau, R.; Dyer, P. W. In *Comprehensive Heterocyclic Chemistry III*; Ramsden, C. A., Scriven, E. F. V., Taylor, R. J. K., Eds.; Elsevier: Oxford, 2008; Chapter 3.15, pp 1029–1048. (c) Matano, Y.; Imahori, H. *Org. Biomol. Chem.* **2009**, *7*, 1258. (d) Fukazawa, A.; Yamaguchi, S. *Chem.—Asian J.* **2009**, *4*, 1386. (e) Ren, Y.; Baumgartner, T. *Dalton Trans.* **2012**, *41*, 7792.

(2) (a) Rausch, M. D.; Klemann, L. P. *J. Am. Chem. Soc.* **1967**, *89*, 5732. (b) Märkl, G.; Jin, G. Y.; Berr, K.-P. *Tetrahedron Lett.* **1993**, *34*, 3103. (c) Trishin, Y. G.; Namestnikov, V. I.; Bel'skii, V. K. *Russ. J. Gen. Chem.* **2004**, *74*, 189. (d) Tsuji, H.; Sato, K.; Ilies, L.; Itoh, Y.; Sato, Y.; Nakamura, E. *Org. Lett.* **2008**, *10*, 2263. (e) Sanji, T.; Shiraishi, K.; Kashiwabara, T.; Tanaka, M. *Org. Lett.* **2008**, *10*, 2689. (f) Fukazawa, A.; Ichihashi, Y.; Kosaka, Y.; Yamaguchi, S. *Chem.—Asian J.* **2009**, *4*, 1729.

(3) (a) Baumgartner, T.; Neumann, T.; Wirges, B. *Angew. Chem., Int. Ed.* **2004**, *43*, 6197. (b) Baumgartner, T.; Bergmans, W.; Kárpáti, T.; Neumann, T.; Nieger, M.; Nyulászi, L. *Chem.—Eur. J.* **2005**, *11*, 4687. (c) Durben, S.; Dienes, Y.; Baumgartner, T. *Org. Lett.* **2006**, *8*, 5893. (d) Ren, Y.; Baumgartner, T. *J. Am. Chem. Soc.* **2011**, *133*, 1328. (e) Ren, Y.; Baumgartner, T. *Inorg. Chem.* **2012**, *51*, 2669 and references therein.

(4) (a) Chen, R.-F.; Zhu, R.; Fan, Q.-L.; Huang, W. *Org. Lett.* **2008**, *10*, 2913. (b) Zhang, S.; Chen, R.; Yin, J.; Liu, F.; Jiang, H.; Shi, N.; An, Z.; Ma, C.; Liu, B.; Huang, W. *Org. Lett.* **2010**, *12*, 3438.

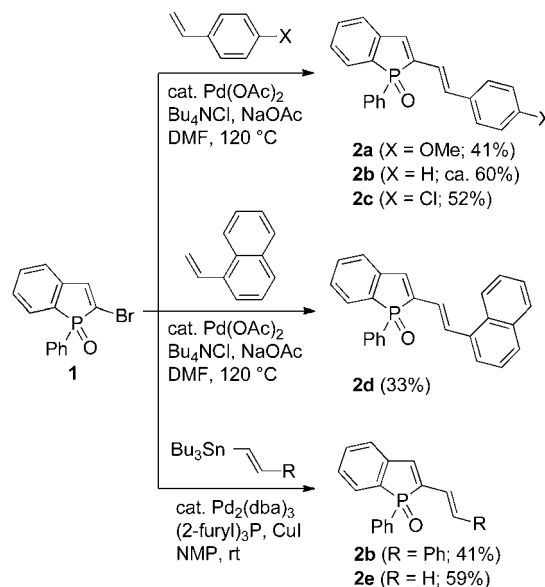
exhibit extremely high emitting abilities and/or high electron drift mobilities in the amorphous state.

Most of the benzo[*b*]phosphole derivatives have been prepared by means of cycloaddition reactions of 2-alkynylphenyl(aryl)phosphines.<sup>3,8,9</sup> In this type of transformation,  $\pi$ -conjugative substituents should be incorporated into starting materials; it is necessary to prepare a 2-alkynylphenyl(aryl)phosphine for each benzo[*b*]phosphole. In 2012, we reported a new divergent method for the  $\alpha$ -functionalization of a benzo[*b*]phosphole skeleton,<sup>10</sup> which was based on Stille coupling reactions of 2-bromobenzo[*b*]phosphole *P*-oxide<sup>11</sup> (**1**, in Scheme 1) with 2-stannylbenzo[*b*]heteroles. It was found that the benzo[*b*]phosphole–indole hybrid was highly fluorescent with large charge-transfer (CT) character in the excited state.<sup>10</sup> To our knowledge, however, the kind of  $\pi$ -conjugative substituents that have been introduced to the  $\alpha$  position of the benzo[*b*]phosphole skeleton is still limited. Therefore, we have applied cross-coupling strategies to the syntheses of new kinds of  $\pi$ -extended benzo[*b*]phosphole derivatives. Herein, we report a series of 2-alkenyl- and 2-alkynyl-benzo[*b*]phospholes, which are available from **1** by using Stille, Heck, or Sonogashira reactions. The electronic effects of the vinylene/acetylene spacers and the *para*-substituents on the optical properties of the newly constructed  $\pi$ -systems are discussed comparatively. Furthermore, the C–Sn cross-coupling of **1** was applied to the facile synthesis of a new Stille-coupling precursor, 2-stannylbenzo[*b*]phosphole.

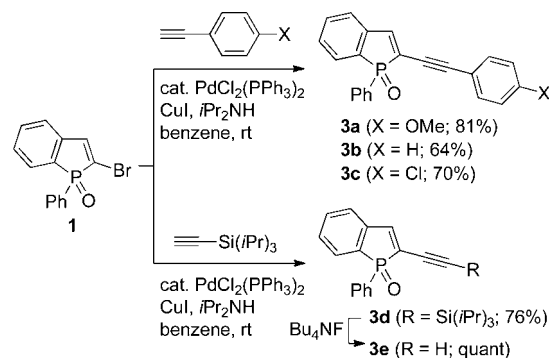
Scheme 1 summarizes the synthesis of 2-alkenylbenzo[*b*]phosphole *P*-oxides **2**. Treatment of the bromide **1** with four kinds of vinylarenes under a standard Heck condition [Pd(OAc)<sub>2</sub>, Bu<sub>4</sub>NCl, NaOAc, DMF at 120 °C] gave the corresponding 2-((*E*)-2-arylethenyl)benzo[*b*]phosphole *P*-oxides **2a–d** as the major products. The introduction of vinyl groups was also achieved by Stille coupling reactions of **1** with alkenyl(tributyl)stannanes, affording **2b** and **2e** in 41–59% yields. The bromide **1** also reacted with three kinds of arylacetylenes and triisopropylsilylacetylene under a standard Sonogashira condition [Pd, CuI, *i*Pr<sub>2</sub>NH, benzene at room temperature] to give the corresponding

2-alkynylbenzo[*b*]phosphole *P*-oxides **3a–d** in 64–81% yields (Scheme 2). The triisopropylsilyl group of **3d** was easily removed by treatment with Bu<sub>4</sub>NF, generating the terminal free 2-ethynylbenzo[*b*]phosphole *P*-oxide **3e** in quantitative NMR yield.

**Scheme 1.** Synthesis of 2-Alkenylbenzo[*b*]phosphole *P*-Oxides



**Scheme 2.** Synthesis of 2-Alkynylbenzo[*b*]phosphole *P*-Oxides



The 2-substituted benzo[*b*]phosphole *P*-oxides **2** and **3** were characterized by using conventional spectroscopic techniques (NMR, HRMS, IR). The <sup>31</sup>P NMR peaks of **2** and **3** appeared at  $\delta_P$  = 31.5–33.3 and 34.5–35.5 ppm, respectively. The structures of **2b–d** and **3b,c** were unambiguously elucidated by X-ray crystallography (Figures 1 and S1 in the Supporting Information).<sup>12</sup> The styryl derivatives **2b,c** possess highly planar frameworks with torsion angles at the inter-ring linkage (C1–C9–C10–C11) of ca. 179°, whereas the 2-(1-naphthyl)ethenyl derivative **2d** and the aryethynyl derivatives **3b,c** display twisted  $\pi$ -networks probably due to the crystal packing effects. In the crystalline states of **2b–d**, the vinylene-linked

(5) (a) Fukazawa, A.; Hara, M.; Okamoto, T.; Son, E.-C.; Xu, C.; Tamao, K.; Yamaguchi, S. *Org. Lett.* **2008**, *10*, 913. (b) Fukazawa, A.; Yamada, H.; Yamaguchi, S. *Angew. Chem., Int. Ed.* **2008**, *47*, 5582. (c) Bruch, A.; Fukazawa, A.; Yamaguchi, E.; Yamaguchi, S.; Studer, A. *Angew. Chem., Int. Ed.* **2011**, *50*, 12094. (d) Fukazawa, A.; Yamaguchi, E.; Ito, E.; Yamada, H.; Wang, J.; Irle, S.; Yamaguchi, S. *Organometallics* **2011**, *30*, 3870.

(6) (a) Nakano, K.; Oyama, H.; Nishimura, Y.; Nakasako, S.; Nozaki, K. *Angew. Chem., Int. Ed.* **2012**, *51*, 695. (b) Yavari, K.; Moussa, S.; Hassine, B. B.; Retailleau, P.; Voituriez, A.; Marinetti, A. *Angew. Chem., Int. Ed.* **2012**, *51*, 6748.

(7) Weymiers, W.; Zaal, M.; Slootweg, J. C.; Ehlers, A. W.; Lammertsma, K. *Inorg. Chem.* **2011**, *50*, 8516.

(8) Aitken, R. A. In *Science of Synthesis*; Maas, G., Ed.; Georg Thieme Verlag: Stuttgart, 2001; Vol. 10, Chapter 10.17–19, pp 789–838.

(9) (a) Winter, W. *Tetrahedron Lett.* **1975**, *16*, 3913. (b) Winter, W. *Chem. Ber.* **1977**, *110*, 2168. (c) Butters, T.; Winter, W. *Chem. Ber.* **1984**, *117*, 990.

(10) Hayashi, Y.; Matano, Y.; Suda, K.; Kimura, Y.; Nakao, Y.; Imahori, H. *Chem.—Eur. J.* **2012**, *18*, 15972.

(11) Nief, F.; Charrier, C.; Mathy, F.; Simalty, M. *Phosphorus, Sulfur Silicon Relat. Elem.* **1982**, *13*, 259.

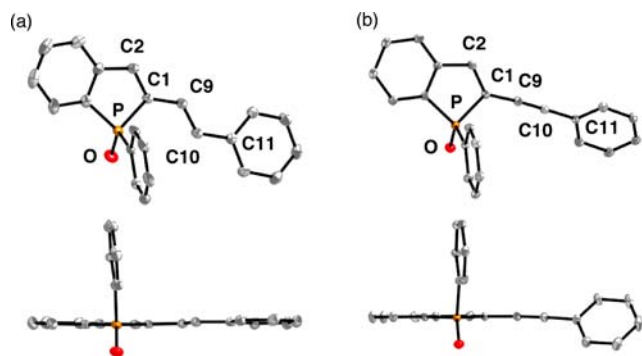


**Figure 1.** Crystal structures of (a) **2b** and (b) **3b**: Top views (upper) and side views (lower). Selected bond lengths (Å), bond angles (deg), and torsion angles (deg): **2b**: P–O, 1.4859(10); C1–C2, 1.3510(19); C1–C9, 1.4414(19); C9–C10, 1.3421(19); C10–C11, 1.466(2); C1–C9–C10, 125.43(12); C9–C10–C11, 125.79(13); C2–C1–C9–C10, 177.03(13); C1–C9–C10–C11, 178.81(12). **3b**: P–O, 1.4827(8); C1–C2, 1.3499(16); C1–C9, 1.4196(16); C9–C10, 1.2013(17); C10–C11, 1.4375(17); C1–C9–C10, 175.93(12); C9–C10–C11, 178.07(13).

$\pi$ -networks are partially stacked with the  $\pi$ – $\pi$  distances of 3.4–3.5 Å.

To understand the effects of the *para*-substituents and the  $\pi$ -spacers (vinylene, acetylene) on the optical and electrochemical properties of benzo[*b*]phosphole *P*-oxides, we measured absorption/emission spectra and redox potentials of **2** and **3** in  $\text{CH}_2\text{Cl}_2$ . The results are summarized in Figure 2 and Table 1. All the compounds examined are moderately to highly fluorescent in solution. In each series of the *para*-substituted derivatives (**2a–c** and **3a–c**), the absorption maxima ( $\lambda_{\text{ab}}$ ) and emission maxima ( $\lambda_{\text{em}}$ ) shift to longer wavelength with increasing the electron donating ability of the *para* substituents on the terminal benzene ring. In each series, the red shifts of the emission maxima are larger than those of the absorption maxima, suggesting that the excited singlet ( $S_1$ ) states are more sensitive than the ground states to the *para*-substituent effects. In addition, the solvatochromism of the fluorescence spectra was

**Table 1.** Optical Data and Redox Potentials of **2** and **3** in  $\text{CH}_2\text{Cl}_2$

compd	$\lambda_{\text{ab}}/\text{nm}$ (log $\epsilon$ )	$\lambda_{\text{em}}/\text{nm}^a$ ( $\Phi_{\text{F}}^b$ )	$E_{\text{ox}}/\text{V}^c$	$E_{\text{red}}/\text{V}^c$
<b>2a</b>	383 (4.31)	469 (0.73)	+0.77	–2.12
<b>2b</b>	367 (4.30)	446 (0.66)	+1.04	–2.07
<b>2c</b>	369 (4.40)	447 (0.60)	+1.12	–2.03
<b>2d</b>	376 (4.63)	468 (0.70)	+0.97	–2.05
<b>2e</b>	339 (3.79)	408 (0.81)	n.d.	–2.23
<b>3a</b>	374 (4.39)	455 (0.65)	+1.08	–2.02
<b>3b</b>	362 (4.25)	434 (0.77)	n.d.	–1.96
<b>3c</b>	361 (4.30)	437 (0.71)	n.d.	–1.95
<b>3d</b>	347 (3.97)	418 (0.69)	n.d.	–2.06

<sup>a</sup> Excited at  $\lambda_{\text{ab}}$ . <sup>b</sup> Absolute fluorescence quantum yields. <sup>c</sup> First oxidation ( $E_{\text{ox}}$ ) and reduction ( $E_{\text{red}}$ ) potentials (vs  $\text{Fc}/\text{Fc}^+$ ) determined by DPV (0.1 M  $\text{Bu}_4\text{N}^+\text{PF}_6^-$ ;  $\text{Ag}/\text{Ag}^+$ ). n.d. = Not determined.

clearly observed for **2a–c** and **3a–c**, in which Stokes shifts increase with the increase of solvent polarity (Figures S2 and S3, Supporting Information). It should be noted that the changes in Stokes shifts of the *para*-methoxy derivatives (**2a** and **3a**) are larger than those of the *para*-chloro derivatives (**2c** and **3c**). Apparently, the CT character in the  $S_1$  states of 2-alkenyl- and 2-alkynyl-benzo[*b*]phosphole *P*-oxides are appreciably enhanced when combined with the electron-donating *para*-methoxyphenyl groups; the benzo[*b*]phosphole unit behaves as the electron-accepting function. The  $\lambda_{\text{ab}}$  and  $\lambda_{\text{em}}$  values as well as the degree of solvatochromism ( $\Delta\lambda_{\text{em}} = 1250 \text{ cm}^{-1}$ ) observed for **2a** are comparable to those for **3a** ( $\Delta\lambda_{\text{em}} = 1250 \text{ cm}^{-1}$ ), suggesting that the linkage effects of the vinylene and acetylene spacers on the  $\pi$ -conjugation are close to each other. The electrochemical redox processes of **2** and **3** were measured by cyclic voltammetry (CV) and differential pulse voltammetry (DPV). In the CV measurements, irreversible CV waves were observed for both oxidation and reduction processes (Figure S4, Supporting Information). As shown in Table 1, the *para*-substituents affect the oxidation potentials ( $E_{\text{ox}}$ ) more efficiently than the reduction potentials ( $E_{\text{red}}$ ). This is consistent with theoretical prediction (B3LYP/6-31G\*); the orbital coefficient at the *para* carbon in HOMO is more distinct than that in LUMO (Figure S7, Supporting Information). The differences in the redox potentials ( $E_{\text{ox}} - E_{\text{red}}$ ) increase in the order, **2a** (2.89 V) < **2b** (3.11 V) < **2c** (3.15 V) for the vinylene-linked series, which agrees well with the order of their HOMO–LUMO gaps obtained by the DFT calculations.

To attain some insight into excited-state dynamics of the newly constructed  $\pi$ -systems, we measured fluorescence lifetimes ( $\tau_{\text{f}}$ ) of **2a–e** and **3a–c** in  $\text{CH}_2\text{Cl}_2$  at room temperature. The  $\tau_{\text{f}}$  values of the styryl derivatives **2a–d** (2.7–3.7 ns) are comparable to those of the aryethynyl derivatives **3a–c** (3.0–3.9 ns). The radiative and non-radiative decay rate constants ( $k_{\text{r}}$  and  $k_{\text{nr}}$ ) calculated from  $\tau_{\text{f}}$  and  $\Phi_{\text{F}}$  values are summarized in Table S2 in the Supporting Information. Among **2a–c** and **3a–c**, the effects of *para* substituents and  $\pi$ -spacers on the  $k_{\text{r}}$  values ( $1.9$ – $2.4 \times 10^8 \text{ s}^{-1}$ ) are negligible compared to those on the  $k_{\text{nr}}$  values ( $0.6$ – $1.5 \times 10^8 \text{ s}^{-1}$ ), although the absolute values

(12) **2b**:  $\text{C}_{22}\text{H}_{17}\text{OP}$ , MW = 328.33,  $0.30 \times 0.25 \times 0.10 \text{ mm}$ , monoclinic,  $P2_1/c$ ,  $a = 9.308(2) \text{ Å}$ ,  $b = 11.131(2) \text{ Å}$ ,  $c = 17.312(4) \text{ Å}$ ,  $\beta = 103.927(3)^\circ$ ,  $V = 1741.0(6) \text{ Å}^3$ ,  $Z = 4$ ,  $\rho_{\text{calcd}} = 1.253 \text{ g cm}^{-3}$ ,  $\mu = 1.62 \text{ cm}^{-1}$ , collected 13447, independent 3943, parameters 217,  $R_w = 0.0914$ ,  $R = 0.0395$  ( $I > 2\sigma(I)$ ), GOF = 1.053. **2c**:  $\text{C}_{22}\text{H}_{16}\text{ClOP}$ , MW = 362.77,  $0.40 \times 0.15 \times 0.10 \text{ mm}$ , monoclinic,  $P2_1/n$ ,  $a = 6.3504(2) \text{ Å}$ ,  $b = 7.9511(3) \text{ Å}$ ,  $c = 35.8818(12) \text{ Å}$ ,  $\beta = 94.457(2)^\circ$ ,  $V = 1806.29(11) \text{ Å}^3$ ,  $Z = 4$ ,  $\rho_{\text{calcd}} = 1.334 \text{ g cm}^{-3}$ ,  $\mu = 3.06 \text{ cm}^{-1}$ , collected 14141, independent 4142, parameters 226,  $R_w = 0.0956$ ,  $R = 0.0381$  ( $I > 2\sigma(I)$ ), GOF = 1.058. **2d**:  $\text{C}_{26}\text{H}_{19}\text{OP}$ , MW = 378.38,  $0.35 \times 0.20 \times 0.15 \text{ mm}$ , monoclinic,  $P2_1/c$ ,  $a = 8.3951(13) \text{ Å}$ ,  $b = 8.9874(13) \text{ Å}$ ,  $c = 25.691(4) \text{ Å}$ ,  $\beta = 94.065(3)^\circ$ ,  $V = 1933.5(5) \text{ Å}^3$ ,  $Z = 4$ ,  $\rho_{\text{calcd}} = 1.300 \text{ g cm}^{-3}$ ,  $\mu = 1.56 \text{ cm}^{-1}$ , collected 22777, independent 4418, parameters 253,  $R_w = 0.0917$ ,  $R = 0.0368$  ( $I > 2\sigma(I)$ ), GOF = 1.090. **3b**:  $\text{C}_{22}\text{H}_{15}\text{OP}$ , MW = 326.31,  $0.30 \times 0.25 \times 0.15 \text{ mm}$ , monoclinic,  $P2_1/c$ ,  $a = 7.9918(8) \text{ Å}$ ,  $b = 18.1517(17) \text{ Å}$ ,  $c = 11.7749(12) \text{ Å}$ ,  $\beta = 96.3610(10)^\circ$ ,  $V = 1697.6(3) \text{ Å}^3$ ,  $Z = 4$ ,  $\rho_{\text{calcd}} = 1.277 \text{ g cm}^{-3}$ ,  $\mu = 1.66 \text{ cm}^{-1}$ , collected 13548, independent 3851, parameters 217,  $R_w = 0.0929$ ,  $R = 0.0340$  ( $I > 2\sigma(I)$ ), GOF = 1.039. **3c**:  $\text{C}_{22}\text{H}_{14}\text{ClOP}$ , MW = 360.75,  $0.30 \times 0.20 \times 0.10 \text{ mm}$ , monoclinic,  $P2_1/c$ ,  $a = 9.961(2) \text{ Å}$ ,  $b = 8.7326(17) \text{ Å}$ ,  $c = 21.055(4) \text{ Å}$ ,  $\beta = 102.507(3)^\circ$ ,  $V = 1788.0(6) \text{ Å}^3$ ,  $Z = 4$ ,  $\rho_{\text{calcd}} = 1.340 \text{ g cm}^{-3}$ ,  $\mu = 3.09 \text{ cm}^{-1}$ , collected 13927, independent 4054, parameters 226,  $R_w = 0.0912$ ,  $R = 0.0344$  ( $I > 2\sigma(I)$ ), GOF = 1.044.

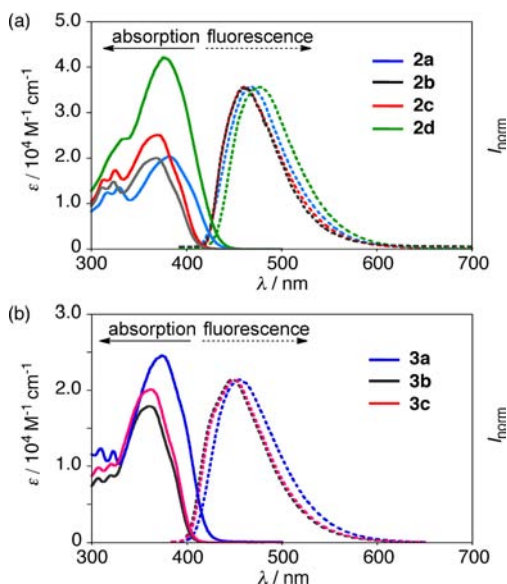


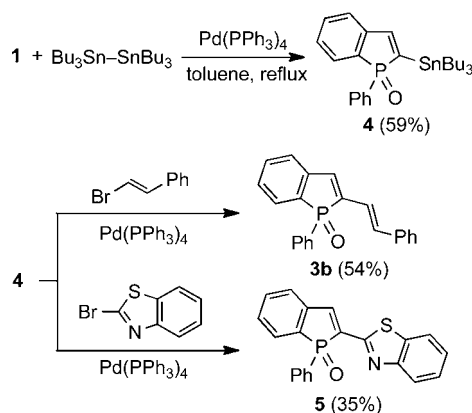
**Figure 2.** UV–vis absorption (dashed line) and emission spectra (dotted line, excited at the absorption maxima) of **2a–d** (a) and **3a–c** (b) in  $\text{CH}_2\text{Cl}_2$ .

of their differences are small. It is worth noting that the attachment of the phenyl group onto the vinyl function (**2a** vs **2e**) appreciably enhances the  $k_{\text{nr}}$  value ( $9.7 \times 10^7$  vs  $2.0 \times 10^7 \text{ s}^{-1}$ ). More efficient internal conversion and/or intersystem crossing with the increased vibrational mode as well as photochemical reactions may account for the acceleration of nonradiative decay from the  $\text{S}_1$  state of **2a–d**.<sup>13</sup>

Furthermore, we conducted a Pd-catalyzed C–Sn cross-coupling reaction of **1** with hexabutyldistannane to obtain 2-stannylbenzo[*b*]phosphole *P*-oxide **4** as a new common precursor for Stille coupling reactions (Scheme 3). The desired stannylation occurred slowly under the Pd catalysis at reflux in toluene to give **4** in 59% yield. Subsequently, the 2-stannyl derivative **4** underwent Stille coupling with  $\beta$ -bromostyrene and 2-bromobenzothiazole to yield **3b** and benzo[*b*]phosphole–benzothiazole hybrid **5**,<sup>10</sup> respectively. These are the first examples of the C–C

(13) When irradiated in toluene with a high-pressure Hg arc lamp ( $>360 \text{ nm}$ ) for 1 h in an argon atmosphere, **2b** decomposed to some extent (judged by  $^1\text{H}$  and  $^{31}\text{P}$  NMR spectra).

**Scheme 3.** Synthesis of 2-(Tributylstannyl)benzo[*b*]phosphole **4** and Its Conversion to **3b** and **5**



bond formation starting from 2-stannylbenzo[*b*]phosphole derivative.

In summary, we have established convenient and divergent methods for the synthesis of 2-alkenyl-, 2-alkynyl-, and 2-stannyl-benzo[*b*]phosphole *P*-oxides by using four kinds of cross-coupling reactions of 2-bromobenzo[*b*]phosphole *P*-oxide. The CT character of the vinylene- and acetylene-bridged benzo[*b*]phosphole  $\pi$ -systems in the excited state has proven to vary widely depending on the terminal *para*-substituents. With the present results in hand, a variety of  $\pi$ -conjugated benzo[*b*]phosphole derivatives are conceivable as functional dyes for use in organic electronic devices, and studies along this line are now in progress.

**Acknowledgment.** This work was supported by a Grant-in-Aid (No. 25288020) from the Ministry of Education, Culture, Sports, Science and Technology (MEXT), Japan and Ogasawara foundation. Y.M. and Y.H. deeply thank Prof. Hiroko Yamada (NAIST) for her kind support and valuable suggestions on this research project.

**Supporting Information Available.** Experimental details, crystal structures, spectral data, CIF files, and DFT calculation results. This material is available free of charge via the Internet at <http://pubs.acs.org>.

The authors declare no competing financial interest.